Friction and nonlinearity compensation in hard disk drive servo systems using robust composite nonlinear feedback control *

Kemao Peng, Ben M Chen
Guoyang Cheng & Tong H Lee

Department of Electrical and Computer Engineering
National University of Singapore, Singapore

SUMMARY: This paper presents design of hard disk drive (HDD) servo systems using an enhanced composite nonlinear feedback (CNF) control technique with a simple friction and nonlinearity compensation scheme. Friction and nonlinearity result in large residual errors and deteriorate the performance of head positioning of HDD servo systems. The enhanced CNF technique has a feature of removing the uncompensated portion of friction and nonlinearity without sacrificing the overall tracking performance. Simulation and experimental results for the servo design show that our approach is very effective and successful. In particular, our experimental results show that the enhanced CNF control has outperformed the conventional PID control in settling time. This approach can be adopted to solve other servomechanism problems.

1 INTRODUCTION

The voice-coil-motor (VCM) actuator is widely used in HDDs to actuate a carriage and move a read/write (R/W) head onto a desired track on the platter to read or write data. The R/W head is driven to rotate through a rotary pivot bearing where disturbances such as friction generate. A data flex cable connected with the R/W head through the metal arm is used to transfer data from or to the R/W head. The characteristics of the data flex cable are a highly nonlinear function of the relative displacement of the R/W head. Such nonlinearities, if left uncompensated, deteriorate the performance of the overall HDD servo system.

In the disk drive industry, it persists in need for companies to come up with devices that are cheaper and able to store more data and retrieve or write to them at faster speed. Decreasing the data track width in the HDDs is the current trend to achieve these objectives. Unfortunately, friction disturbances and nonlinearities resulted from the data flex cable and rotary pivot bearing are becoming a bottle neck for such improvement. The issue becomes more noticeable for smaller HDDs. Reducing effect of these disturbances and uncertainties has been one of challenges in designing head positioning servo systems. Much attention has been paid to the research of mitigation of the friction in the rotary pivot bearing in disk drive industry through the 1990s.[1,2,3] It is still ongoing in the disk drive industry.[4,5,6]

In this paper, we will focus on design of HDD servo systems based on the framework of the CNF control, but with the introduction of some additional features to compensate the friction disturbances and nonlinearities. The obtained results show a big improvement over those without such compensation. The paper is organized as follows. A comprehensive model of the actuator of a micro-drive will be presented in Section 2. The theoretical framework of the CNF control law with additional feature to compensate the friction forces and nonlinearities will be derived in Section 3, whereas its application to a micro-drive servo system design will be given in Section 4 together with simulation and experimental results. Finally, some concluding remarks will be drawn in Section 5.

* Paper presented at the Asian Control Conference, Melbourne, 2004.

2 MODEL OF A MICRO-DRIVE

A comprehensive model of a commercial micro-HDD servo system in[7] is chosen to illustrate our theoretical framework and carry out our servo system design and simulation throughout the paper. A typical VCM actuator consists of a coil, a pivot and a metal arm that carries the R/W head. The stator of the VCM motor is made of a permanent magnet. The range of the rotor is typically constrained up to 0.5 rad. The motor is driven by a driver, a full bridge power amplifier to convert the input voltage into electric current, which drives the coil. Examining through the detailed analysis of physical effects together with the Monte Carlo process, Peng *et al.*[7] has recently obtained a fairly comprehensive model of the HDD actuator dynamics, and pivot bearing friction forces as well as the characteristics of the data flex cable. The dynamics of the actuator of an IBM DMDM-10340 at low frequency region is as follows,

$$\ddot{y} = 2.35\times 10^{8}u - 6.78445\times 10^{6}\arctan(0.5886y) + \tilde{T}_f, \tag{1}$$

where

$$\tilde{T}_f = \begin{cases} -(|1.175\times 10^{6}uy + 0.01\dot{y}^2| + 1.5\times 10^{4})\operatorname{sgn}(\dot{y}) - 282.6\dot{y}, & \dot{y}\neq 0, \\ -\tilde{T}_e, & \dot{y}=0, |\tilde{T}_e| \le \tilde{T}_s, \\ -\tilde{T}_s\operatorname{sgn}(\tilde{T}_e), & \dot{y}=0, |\tilde{T}_e| > \tilde{T}_s, \end{cases}$$

$$\tilde{T}_e = 2.35\times 10^{8}[-0.02887\arctan(0.5886y) + u],$$
$$\tilde{T}_s = 1.293\times 10^{6}|u_0 y_0| + 1.65\times 10^{4}, \tag{2}$$

with u_0 and y_0 being respectively the corresponding input voltage and the R/W head displacement for the case when $\dot{y}=0$. The high frequency resonant modes are given by

$$\begin{aligned} G_{rm}(s) = {} & \frac{0.8709s^2 + 1726s + 1.369\times 10^9}{s^2 + 1480s + 1.369\times 10^9} \times \frac{0.9332s^2 - 805.8s + 1.739\times 10^9}{s^2 + 125.1s + 1.739\times 10^9} \\ & \times \frac{1.072s^2 + 925.1s + 1.997\times 10^9}{s^2 + 536.2s + 1.997\times 10^9} \times \frac{0.9594s^2 + 98.22s + 2.514\times 10^9}{s^2 + 1805s + 2.514\times 10^9} \\ & \times \frac{7.877\times 10^9}{s^2 + 6212s + 7.877\times 10^9}. \end{aligned} \tag{3}$$

The overall VCM actuator model is composed of (1) to (3). The input signal to the actuator, u, in V, is bounded ±3V. The displacement of the actuator, y, has a unit of micrometer. Generally, for large drives, these friction forces and data flex cable nonlinearities are negligible. However, for micro drives, these disturbances and nonlinearities would yield a significant bias and large residual error, and deteriorate performance of the overall servo system. A special treatment is needed to reduce the effect of these disturbances and uncertainties, which is the focus of the coming sections.

3 ENHANCED CNF CONTROL TECHNIQUE

An enhanced version of CNF control design will be presented in this section, which is capable of removing constant bias in servo systems. The original CNF technique[8,9,10] is applicable to systems with input saturation but without external disturbances. When the given system has disturbances, the resulting system output generally does not asymptotically match the target reference without knowing *a priori* the level of bias. A common approach for removing bias resulting from constant disturbances is to add an integrator to the controller. We propose in this section an enhanced CNF design scheme by introducing an additional integration action in the design. The new approach will retain the fast rise time property of the original CNF control and at the same have an additional capacity of eliminating steady state bias due to disturbances. More specifically, we consider a linear system with an amplitude constrained actuator, characterized by

$$\begin{cases} \dot{x} = Ax + B\operatorname{sat}(u) + Ew, & x(0) = x_0, \\ y = C_1 x, \\ h = C_2 x, \end{cases} \tag{4}$$

where $x\in\Re^n$, $u\in\Re$, $y\in\Re^p$, $h\in\Re$ and $w\in\Re$ are respectively the state, control input, measurement output, controlled output and disturbance input of the system. A, B, C_1, C_2 and E are appropriate dimensional constant matrices. The function, $\text{sat}: \Re \to \Re$, represents the actuator saturation defined as

$$\text{sat}(u) = \text{sgn}(u)\min\{u_{\max}, |u|\}, \tag{5}$$

with $u_{\max}$ being the saturation level of the input. The assumptions on the given system are made:

1) (A, B) is stabilizable,
2) (A, C_1) is detectable,
3) (A, B, C_2) is invertible and has no invariant zero at $s = 0$,
4) w is bounded unknown constant disturbance, and
5) h is a subset of y, *i.e.*, h is also measurable.

Note that all these assumptions are fairly standard for tracking control. We aim to design an enhanced CNF control law for the system with disturbances such that the resulting controlled output would track a target reference (set point), say r, as fast and as smooth as possible without steady state error. We first follow the usual practice to augment an integrator into the given system. Such an integrator will eventually become part of the final control law. To be more specific, we define an auxiliary state variable,

$$\dot{z} = e := h - r = C_2 x - r, \tag{6}$$

which is implementable as is assumed to be measurable, and augment it into the given system as follows,

$$\begin{cases} \dot{\bar{x}} = \bar{A}\bar{x} + \bar{B}\,\text{sat}(u) + \bar{B}_r r + \bar{E}w, \\ \bar{y} = \bar{C}_1 \bar{x}, \\ h = \bar{C}_2 \bar{x}, \end{cases} \tag{7}$$

$$\bar{x} = \begin{pmatrix} z \\ x \end{pmatrix},\quad \bar{x}_0 = \begin{pmatrix} 0 \\ x_0 \end{pmatrix},\quad \bar{y} = \begin{pmatrix} z \\ y \end{pmatrix},\quad \bar{A} = \begin{bmatrix} 0 & C_2 \\ 0 & A \end{bmatrix},$$

$$\bar{B} = \begin{bmatrix} 0 \\ B \end{bmatrix},\quad \bar{B}_r = \begin{bmatrix} -1 \\ 0 \end{bmatrix}, \tag{8}$$

and

$$\bar{E} = \begin{bmatrix} 0 \\ E \end{bmatrix},\quad \bar{C}_1 = \begin{bmatrix} 1 & 0 \\ 0 & C_1 \end{bmatrix},\quad \bar{C}_2 = \begin{bmatrix} 0 & C_2 \end{bmatrix}. \tag{9}$$

We note that under Assumptions 1 and 3, the pair $(\bar{A}, \bar{B})$ is stabilizable. This can be justified by considering the rank property of the related matrices. Next, we proceed to carry out the design of enhanced CNF control laws for two different cases, *i.e.*, the state feedback case and the reduced order measurement feedback case. The full order measurement feedback case is straightforward once the result for the reduced order case is established. We note that the procedure for designing the enhanced CNF control laws is a natural extension of that of [8,9]. The enhanced control laws are, however, capable of removing steady state bias.

3.1 State feedback case

We first investigate the case when all the state variables of the plant (7) are measurable, *i.e.*, $\bar{y} = \bar{x}$. The procedure that generates an enhanced CNF state feedback law will be done in three steps. That is, in the first step, a linear feedback control law will be designed, in the second step, the design of nonlinear feedback control will be carried out, and lastly, in the final step, the linear and nonlinear feedback laws will be combined to form an enhanced CNF control law.

Step 3.S.1: Design a linear feedback control law,

$$u_L = F\,\bar{x} + G\,r, \tag{10}$$

where F is chosen such that

1) $\bar{A} + \bar{B}F$ is an asymptotically stable matrix, and
2) The closed-loop system $\bar{C}_2(sI - \bar{A} - \bar{B}F)^{-1}\bar{B}$ has certain desired properties.

Let us partition

$$F = \begin{bmatrix} F_z & F_x \end{bmatrix}, \tag{11}$$

in conformity with z and x. The general guideline in design such an is to place the closed-loop pole of $\bar{A} + \bar{B}F$ corresponding to the integration mode, z, to be sufficiently closer to the imaginary axis compared to the rest eigenvalues, which implies that F_z is a relatively small scalar. The remaining closed-loop poles of $\bar{A} + \bar{B}F$ should be placed to have a dominating pair with a small damping ratio, which in turn would yield a fast rise time in the closed-loop system response. Finally, G is chosen as

$$G = -[C_2(A + BF_x)^{-1}B]^{-1}, \tag{12}$$

which is well defined as (A, B, C_2) is assumed to have no invariant zeros at $s = 0$ and $A + BF_x$ is nonsingular whenever $\bar{A} + \bar{B}F$ is stable and F_z is relatively small.

Step 3.S.2: Given a positive definite symmetric matrix $W \in \Re^{(n+1)\times(n+1)}$, we solve the following Lyapunov equation:

$$(\bar{A}+\bar{B}F)'P+P(\bar{A}+\bar{B}F)=-W. \tag{13}$$

Such a solution $P>0$ is always existent as $\bar{A}+\bar{B}F$ is asymptotically stable. The nonlinear feedback portion of the enhanced CNF control law, u_N, is given by

$$u_N=\rho(e)\bar{B}'P(\bar{x}-\bar{x}_e), \tag{14}$$

where $\rho(e)$, with $e=h-r$ being the tracking error, is a smooth, non-positive and non-decreasing function of $|e|$, to be used to gradually change the system closed-loop damping ratio to yield a better tracking performance. The procedures for selecting the design parameter W and the nonlinear gain $\rho(e)$ for the enhanced CNF control laws are the same as those for the usual CNF design given.[9] Next, we define

$$G_e:=\begin{bmatrix}0\\-(A+BF_x)^{-1}BG\end{bmatrix},\quad \bar{x}_e:=G_e r. \tag{15}$$

Step 3.S.3: The linear feedback control law and nonlinear feedback portion derived in the previous steps are combined to form an enhanced CNF control law,

$$u=u_L+u_N=F\bar{x}+Gr+\rho(e)\bar{B}'P(\bar{x}-\bar{x}_e). \tag{16}$$

We have the following result.

Theorem 3.1: Consider the given system (4) with $y=x$ and the disturbance w being bounded by a non-negative scalar τ_w, *i.e.*, $|w|\le\tau_w$. Let

$$\gamma:=2\tau_w\lambda_{\max}(PW^{-1})(\bar{E}'P\bar{E})^{1/2}. \tag{17}$$

Then, for any $\rho(e)$, which is a smooth, non-positive and non-decreasing function of $|e|$, the enhanced CNF control law (16) will drive the system controlled output h to track the step reference of amplitude r from an initial state $\bar{x}_0$ asymptotically without steady state error, provided that the following conditions are satisfied:

(i) There exist positive scalars $\delta\in(0,1)$ and $c_\delta>\gamma^2$ such that

$$\forall\bar{x}\in X(F,c_\delta):=\{\bar{x}:\bar{x}'P\bar{x}\le c_\delta\}\Rightarrow|F\bar{x}|\le(1-\delta)u_{\max}, \tag{18}$$

(ii) The initial condition, $\bar{x}_0$ and the level of the target reference, r, satisfy

$$\bar{x}_0-\bar{x}_e\in X(F,c_\delta),\quad |Hr|\le\delta\,u_{\max}, \tag{19}$$

where $H:=FG_e+G$.

3.2 Measurement feedback case

It is unrealistic to assume that all the state variables of a given plant to be measurable. An enhanced CNF control law using only information measurable from the plant will be derived. For simplicity of presentation, we assume that C_1 in the measurement output of the given plant (4) is already in the form,

$$C_1=\begin{bmatrix}I_p & 0\end{bmatrix}, \tag{20}$$

and the augmented plant (7) can then be partitioned as the following:

$$\begin{cases}\begin{pmatrix}\dot{z}\\\dot{x}_1\\\dot{x}_2\end{pmatrix}=\begin{bmatrix}0 & C_{21} & C_{22}\\0 & A_{11} & A_{12}\\0 & A_{21} & A_{22}\end{bmatrix}\begin{pmatrix}z\\x_1\\x_2\end{pmatrix}+\begin{bmatrix}0\\B_1\\B_2\end{bmatrix}\mathrm{sat}(u)+\begin{bmatrix}-1\\0\\0\end{bmatrix}r+\begin{bmatrix}0\\E_1\\E_2\end{bmatrix}w,\\ \bar{y}=\begin{bmatrix}1 & 0 & 0\\0 & I_p & 0\end{bmatrix}\begin{pmatrix}z\\x_1\\x_2\end{pmatrix},\\ h=\begin{bmatrix}0 & C_{21} & C_{22}\end{bmatrix}\begin{pmatrix}z\\x_1\\x_2\end{pmatrix},\end{cases} \tag{21}$$

where

$$\begin{pmatrix}z\\x_1\\x_2\end{pmatrix}=\bar{x},\quad \begin{pmatrix}z(0)\\x_1(0)\\x_2(0)\end{pmatrix}=\begin{pmatrix}0\\x_{10}\\x_{20}\end{pmatrix}=\bar{x}_0,\quad \bar{y}=\begin{pmatrix}z\\y\end{pmatrix}.$$

Clearly, z and $y=x$, are readily available and need not to be estimated. We only need to estimate x_2. There are two main steps in designing a reduced order measurement feedback control laws:

1) The construction of a full state feedback gain matrix F; and
2) The construction of a reduced order observe gain matrix K_R.

The construction of the gain matrix is totally identical to that given in the previous subsection. can be partitioned in conformity with z, x_1 and x_2 as follows,

$$F=\begin{bmatrix}F_z & F_1 & F_2\end{bmatrix}. \tag{22}$$

The reduced order observer gain matrix K_R is chosen such that the poles of $A_{22}+K_RA_{12}$ are placed in appropriate locations in the open-left half plane. The reduced order enhanced CNF control law is given by,

$$\begin{cases} \dot{x}_v = (A_{22}+K_RA_{12})x_v + [A_{21}+K_RA_{11}-(A_{22}+K_RA_{12})K_R]y + (B_2+K_RB_1)\text{sat}(u), \\ u = F\begin{pmatrix} z \\ y \\ x_v - K_Ry \end{pmatrix} + Gr + \rho(e)\overline{B}'P\left[\begin{pmatrix} z \\ y \\ x_v - K_Ry \end{pmatrix} - \overline{x}_e\right], \end{cases} \tag{23}$$

where G is as that defined in (12) and $\rho(e)$ is the smooth, non-positive and non-decreasing function of $|e|$, to be chosen to yield a desired performance. Next, given a positive definite matrix $W \in \Re^{(n+1)\times(n+1)}$, let $\boldsymbol{P} > 0$ be the solution to the Lyapunov equation

$$(\overline{A}+\overline{B}F)'P + P(\overline{A}+\overline{B}F) = -W. \tag{24}$$

Given another positive definite matrix $W_R \in \Re^{(n-p)\times(n-p)}$ with

$$W_R > F_2'\overline{B}'PW^{-1}P\overline{B}F_2, \tag{25}$$

and let $Q_R > 0$ be the solution to the Lyapunov equation

$$(A_{22}+K_RA_{12})'Q_R + Q_r(A_{22}+K_RA_{12}) = -W_R. \tag{26}$$

Note that such P and Q_r exist as $\overline{A}+\overline{B}F$ and $A_{22} + K_RA_{12}$ are both asymptotically stable. We have the following result.

Theorem 3.2 Consider the given system (4) with the disturbance being bounded by a non-negative scalar τ_w, *i.e.*, $|w| \le \tau_w$. Let

$$\gamma_R = 2\tau_w\lambda_{\max}\left(\begin{bmatrix} P & 0 \\ 0 & Q_R \end{bmatrix}\begin{bmatrix} W & -P\overline{B}F_2 \\ -F_2'\overline{B}'P & W_R \end{bmatrix}^{-1}\right)$$
$$[\overline{E}'P\vec{E} + (E_2+K_RE_1)'Q_R(E_2+K_RE_1)]^{1/2}. \tag{27}$$

Then, there exists a scalar $\rho^* > 0$ such that for any $\rho(e)$, a smooth, non-positive and non-decreasing function of $|e|$ with $|\rho(e)| \le \rho^*$, the reduced order enhanced CNF control law of (23) will drive the system controlled output $\boldsymbol{h}$ to track the step reference of amplitude $\boldsymbol{r}$ asymptotically without steady state error, provided that the following conditions are satisfied:

(i) There exist positive scalars $\delta \in (0,1)$ and $c_{R\delta} > \gamma_R^2$ such that

$$\forall \overline{x} \in X(F, c_{R\delta}) := \left\{\overline{x} : \overline{x}'\begin{bmatrix} P & 0 \\ 0 & Q_R \end{bmatrix}\overline{x} \le c_{R\delta}\right\}$$
$$\Rightarrow |[F \quad F_2]\overline{x}| \le (1-\delta)u_{\max}, \tag{28}$$

(ii) The initial conditions, $\overline{x}_0$, $x_{v0} = x_v(0)$ and the level of the target reference, $\boldsymbol{r}$, satisfy

$$\begin{pmatrix} \overline{x}_0 - \overline{x}_e \\ x_{v0} - x_{20} - K_Rx_{10} \end{pmatrix} \in X(F, c_{R\delta}), \quad |Hr| \le \delta u_{\max}, \tag{29}$$

where $\boldsymbol{H}$ is the same as that defined in Theorem 3.1.

4 MICRODRIVE SERVO SYSTEM DESIGN

We proceed to design a servo system for the microdrive identified in Section 2. As mentioned earlier, our design philosophy is rather simple. We will make a full use of the obtained model of the friction and nonlinearities of the VCM actuator to design a pre-compensator, which would cancel as much as possible all the unwanted elements in the servo system. As it is impossible to have perfect models for friction and nonlinearities, a perfect cancellation of these elements is unlikely to happen in the real world. We will then formulate our design by treating the uncompensated portion as external disturbances. The enhanced CNF control technique of Section 3 will then be employed to design an effective tracking controller. The overall control scheme for the servo system is depicted in Figure 1. Although we focus our attention here on HDD, it is our belief that such an approach can be adopted to solve other servo problems.

Examining the model of (1), it is easy to obtain a pre-compensation,

$$u_{pre} = u - \overline{u} = 0.0288737\arctan(0.5886y), \tag{30}$$

which would eliminate the majority of nonlinearities in the data flex cable. The HDD model of (1) can then be simplified as the following:

$$\dot{x} = \begin{bmatrix} 0 & 1 \\ 0 & 0 \end{bmatrix}x + \begin{bmatrix} 0 \\ a \end{bmatrix}\text{sat}(\overline{u}) + \begin{bmatrix} 0 \\ a \end{bmatrix}w, \quad y = h = [1 \quad 0]x, \tag{31}$$

where the disturbance, w, represents uncompensated nonlinearities, $a = 2.35 \times 10^8$ and $\boldsymbol{y}=\boldsymbol{h}$ is the relative

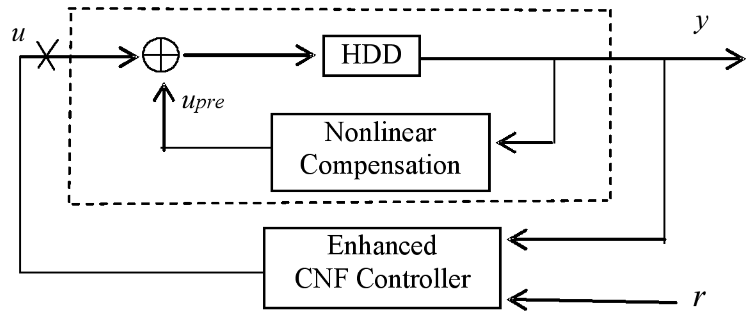

Figure 1: Control scheme for the HDD servo system.

displacement of the R/W head (in micrometer). The control input, $\bar{u}$, is to be limited within $\pm$3V. The corresponding augmented plant to be used in the enhanced CNF design is then given by

$$\begin{cases} \dot{\bar{x}} = \begin{bmatrix} 0 & 1 & 0 \\ 0 & 0 & 1 \\ 0 & 0 & 0 \end{bmatrix} \bar{x} + \begin{bmatrix} 0 \\ 0 \\ a \end{bmatrix} \mathrm{sat}(\bar{u}) + \begin{bmatrix} -1 \\ 0 \\ 0 \end{bmatrix} r + \begin{bmatrix} 0 \\ 0 \\ a \end{bmatrix} w, \\ y = h = \begin{bmatrix} 0 & 1 & 0 \end{bmatrix} \bar{x}. \end{cases} \tag{32}$$

We will focus on our design for $r = 1\mu\mathrm{m}$ in this section, *i.e.*, the track following stage of the HDD servo system. The initial state, $\boldsymbol{x}(0)$, is assumed to be 0. Note that the nonlinearities in the data flex cable and friction do not cause much trouble in the track seeking stage. Following the procedures given in Section 3 and a few simulation tries, we obtain a state feedback gain matrix,

$$F = -\begin{bmatrix} 8.2317\times 10^{-4} & 0.0823 & 2.2459\times 10^{-5} \end{bmatrix} \tag{33}$$

Next, we choose W to be a diagonal matrix with diagonal entries being 7.4536×10^{-4}, 0.0135 and 7.0057×10^{-11}, respectively to solve $P > 0$ from the Lyapunov equation of (13). The reduced order observer gain matrix is selected as $K_R = -6000$ to places the observer pole at -6000, and the nonlinear gain function is selected as follows:

$$\rho(e) = -4.7459[\exp(-|e|) - 0.3679]. \tag{34}$$

Finally, the reduced order enhanced CNF control law for the microdrive servo system is given by

$$\begin{pmatrix} \dot{z} \\ \dot{x}_v \end{pmatrix} = \begin{bmatrix} 0 & 0 \\ 0 & -6000 \end{bmatrix} \begin{pmatrix} z \\ x_v \end{pmatrix} + \begin{bmatrix} 0 \\ a \end{bmatrix} \mathrm{sat}(\bar{u}) + \begin{bmatrix} 1 \\ -3.6\times 10^{7} \end{bmatrix} y + \begin{bmatrix} -1 \\ 0 \end{bmatrix} r, \tag{35}$$

and

$$\bar{u} = \Big(-\begin{bmatrix} 8.2317\times 10^{-4} & 0.0823 & 2.2459\times 10^{-5} \end{bmatrix} + \rho(e)\begin{bmatrix} 0.4527 & 0.0823 & 1.7156\times 10^{-5} \end{bmatrix}\Big) \begin{pmatrix} z \\ y-r \\ x_v + 6000y \end{pmatrix}. \tag{36}$$

To see the effectiveness of the nonlinearity pre-compensation, we design a normal reduced order CNF control law for the original plant without the pre-compensation using the technique reported in[9], which is given by

$$\dot{x}_v = -6000x_v - 3.6\times 10^{7} y + 2.35\times 10^{8}\,\mathrm{sat}(u) \tag{37}$$

and

$$u = \Big(-\begin{bmatrix} 0.0823 & 2.2459\times 10^{-5} \end{bmatrix} + \rho(e)\begin{bmatrix} 0.0823 & 1.7156\times 10^{-5} \end{bmatrix}\Big) \begin{pmatrix} y-r \\ x_v + 6000y \end{pmatrix}, \tag{38}$$

where $\rho(e)$ is the same as that in (34). To compare the result of the enhanced CNF technique with conventional approaches, we design a conventional PID controller,

$$\begin{pmatrix} \dot{z} \\ \dot{x}_d \end{pmatrix} = \begin{bmatrix} 0 & 0 \\ 0 & -10^{5} \end{bmatrix} \begin{pmatrix} z \\ x_d \end{pmatrix} + \begin{bmatrix} 1 \\ 1 \end{bmatrix} (y-r), \tag{39}$$

and

$$\bar{u} = 2.9481(y-r) + 50z + 2.8876\times 10^{5} x_d, \tag{40}$$

for the pre-compensated system. The parameters in (39) and (40) are tuned to yield the best possible implementation result under this control structure.

For simulation, we use the nonlinear model of the HDD in (1) together with all its identified resonance modes given in (3). The simulations are done in a continuous setting, and $|\dot{y}| \le 0.01\mu$ m/s is considered to be 0. The simulation results are shown in Figure 2. Experiments are done on the actual HDD with its cover being removed. The HDD is placed on a vibration-free platform and an LDV is used to measure the displacement of the R/W head of the HDD.

The controllers are implemented using a dSpace DSP installed in a desktop computer. The sampling frequency is set to be 10kHz, a typical sampling frequency used in HDD servo systems. The experimental results are shown in Figure 3. We summarize the tracking performances (in terms of 3% settling time for 40kTPI) in Table 1. Clearly, the performance of the enhanced CNF control is much better than that of the PID control.

Table 1
Settling time (ms): Enhanced CNF versus PID.

Controller	**PID**	**Enhanced CNF**	**Improvement**
Simulation	1.7	0.8	53%
Implementation	4.5	1.1	76%

We next examine the frequency domain properties of the servo system by breaking the loop at the input point to the pre-compensated plant (marked 'X' in Figure 1) and computing its open-loop frequency response with the reference input, *r*, being set to 0.

For the CNF control, which is nonlinear, we replace $\rho(e)$ by $\rho_0 = -3$, representing the steady state situation of such a control scheme. The servo system with the enhanced CNF controller has a gain margin of 7.4 dB and a phase margin of 53°, while the one with the PID controller has a gain margin of 1.6 dB and a phase margin of 68°.

The gain margin in the PID control is not acceptable in practical situations. This could be due to the fact that we have tuned the response of the PID control a bit too fast, although it is very slow compared to that of the enhanced CNF control.

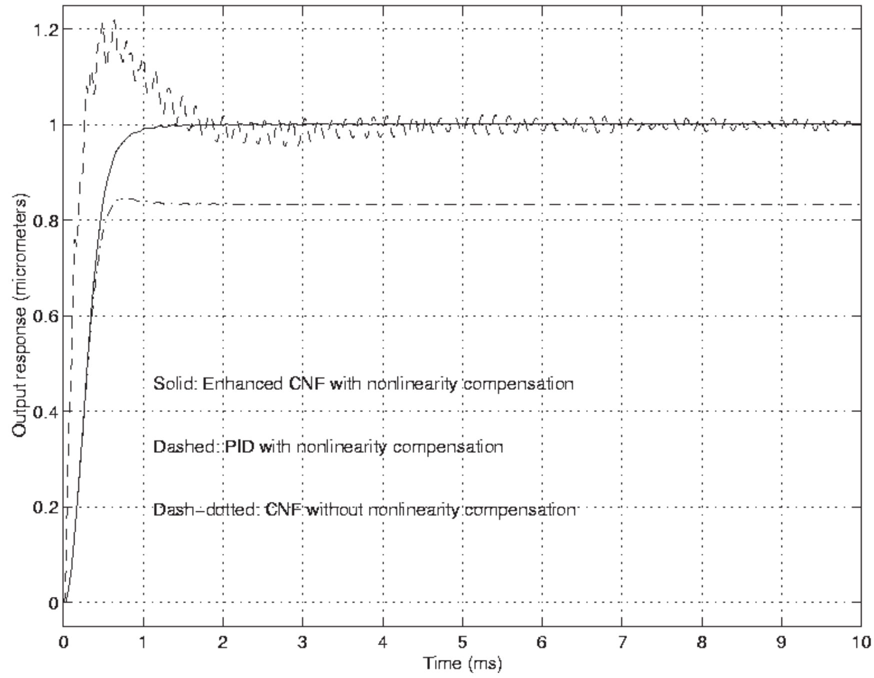

a. Output response.

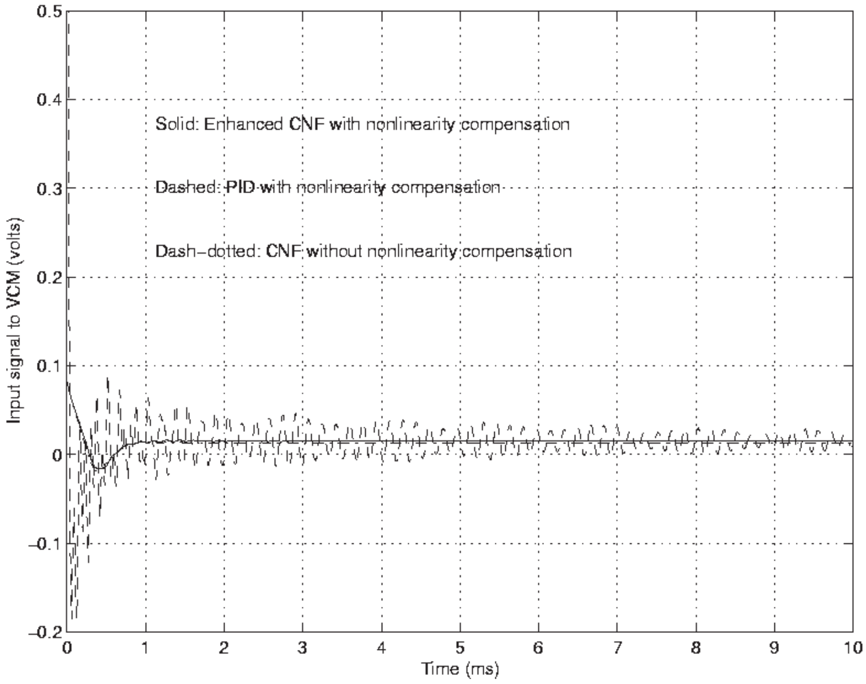

b. Input signal to VCM.

Figure 2: Simulation resutls.

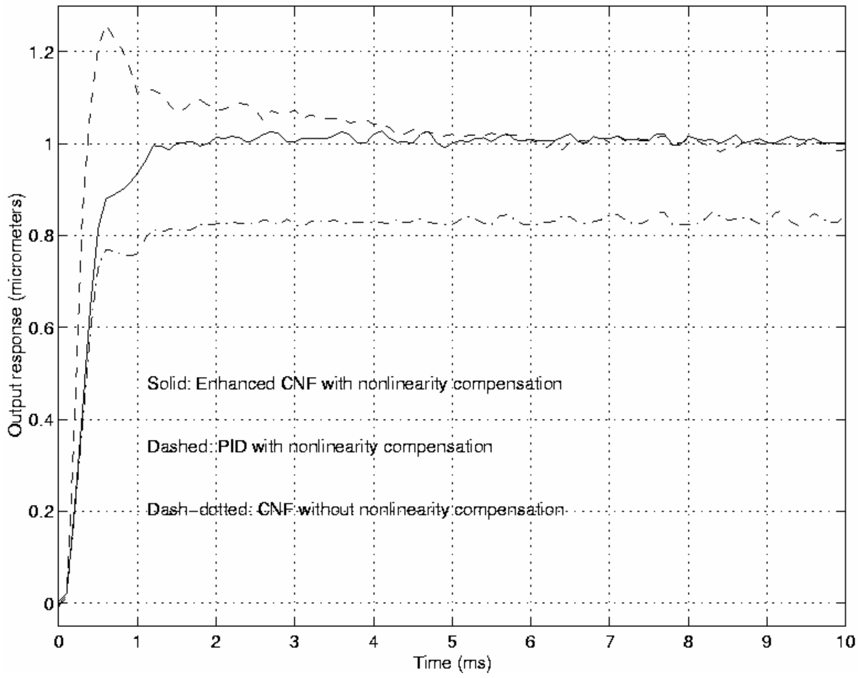

a. Output response.

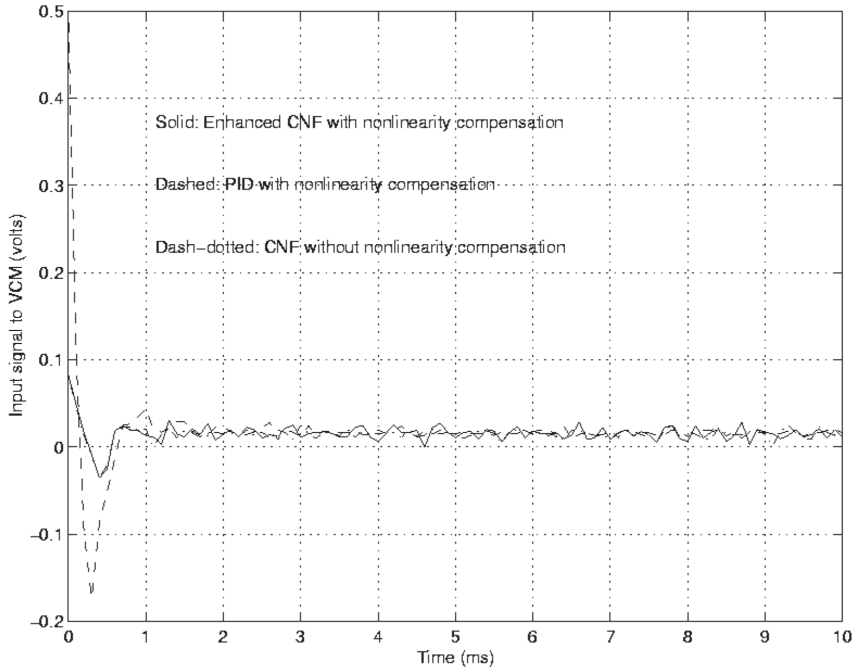

b. Input signal to VCM.

Figure 3: Experimental resutls.

5 CONCLUDING REMARKS

A control structure with a nonlinearity pre-compensation and an enhanced nonlinear composite feedback control technique has been developed and utilized to design a servo system for the microdrive. The simulation and implementation results show that our approach is very efficient and successful. Such a method can be adopted to solve other servomechanism problems.

REFERENCES

1. Abramovitch D, Wang F, Franklin G. Disk drive pivot nonlinearity modelling Part I: frequency domain. In: Proceedings of the 1994 American Control Conference, Baltimore, 1994; 2600-3.

2. Wang F, Hurst T, Abramovitch D, Franklin G. Disk drive pivot nonlinearity modelling Part II: time domain. In: Proceeding of the 1994 American Control Conference, Baltimore, 1994: 2604-7.

3. Wang L, Yuan L, Chen BM, Lee TH. Modeling and control of a dual-stage servo system for hard disk drives. In: Proceedings of the 1998 International Conference on Mechatronic Technology, Hsinchu, Taiwan, 1998: 533-8.

4. Chang HS, Baek SE, Park JH, Byun YK. Modeling of pivot friction using relay function and estimation of its functional parameters. In: Proceeding of the 1999 American Control Conference, San Francisco, 1999: 3784-9.

5. Dammers D, Binet P, Pelz G, Vobkarper LM. Motor modeling based on physical effect models. In: Proceedings of the 2001 IEEE International Workshop on Behavioral Modeling and Simulation, Santa Rosa, California, 2001: 78-83.

6. Liu X, Liu JC. Analysis and measurement of torque hysteresis of pivot bearing in hard disk drive applications. Tribology International, 1999; 32: 125-30.

7. Peng K, Cheng G, Chen BM, Lee TH. Comprehensive modeling of friction in a hard disk drive actuator. In: Proceedings of the 2003 American Control Conference, Denver, June 2003: 1380-5.

8. Chen BM, Lee TH, Venkataramanan V. Hard Disk Drive Servo Systems, New York: Springer, 2002.

9. Chen BM, Lee TH, Peng K, Venkataramanan V. Composite nonlinear feedback control: Theory and an application. IEEE Transactions on Automatic Control, 2003: 48. 427-39.

10. Lin Z, Pachter M, Banda S. Toward improvement of tracking performance -- Nonlinear feedback for linear system. International Journal of Control, 1998; 70: 1-11.